Solid State Communications 152 (2012) 1734–1738

Contents lists available at SciVerse ScienceDirect

Solid State Communications

journal homepage: www.elsevier.com/locate/ssc

Magnetic properties and magnetocaloric effects in $Gd_{1-x}Ho_xNiIn$ intermetallic compounds

H. Zhang [a,*], Z.Y. Xu [a], X.Q. Zheng [a], J. Shen [b], F.X. Hu [a], J.R. Sun [a], B.G. Shen [a,*]

[a] State Key Laboratory for Magnetism, Institute of Physics, Chinese Academy of Sciences, Beijing 100190, PR China
[b] Key laboratory of Cryogenics, Technical Institute of Physics and Chemistry, Chinese Academy of Sciences, Beijing 100190, PR China

ARTICLE INFO

Article history:
Received 10 April 2012
Received in revised form
20 June 2012
Accepted 25 June 2012
by J. Fontcuberta
Available online 6 July 2012

Keywords:
A. Rare-earth compounds
D. Magnetocaloric effect
D. Magnetic entropy change
D. Refrigerant capacity

ABSTRACT

Magnetic properties and magnetocaloric effects (MCEs) of the intermetallic $Gd_{1-x}Ho_xNiIn$ ($x=0-1$) compounds have been evaluated by magnetization and heat capacity measurements. The Curie temperature T_C can be tuned from near 100 K to 20 K by substituting Ho for Gd atoms. In addition, all the compounds with Ho atoms undergo two successive magnetic transitions with the decrease of temperature: a paramagnetic (PM) to ferromagnetic (FM) transition around T_C and a spin-reorientation (SR) transition around $7-9$ K. It is found that both transitions contribute to the magnetic entropy change (ΔS_M). For a field change of 5 T, the maximum values of $-\Delta S_M$ for $Gd_{0.4}Ho_{0.6}NiIn$ are 6 J/kg K at $T_t=9$ K and 10 J/kg K at $T_C=52$ K, respectively. These two $-\Delta S_M$ peaks overlap partly and result in a wide working temperature range of MCE, and thus leading to the largest *RC* value of 443 J/kg in the $Gd_{1-x}Ho_xNiIn$ system.

1. Introduction

Magnetic refrigeration based on the magnetocaloric effect (MCE) has attracted great attention as a promising replacement for the conventional gas compression-expansion technique [1,2]. Recently, many efforts have been made to explore advanced magnetic refrigerant materials suited to domestic or industrial applications near room temperature. However, it has been reported that the research on systems exhibiting large MCEs at low temperature is also important, since these materials are potential magnetic refrigerants for gas liquefaction in fuel industry [2,3]. Therefore, it is strongly desirable to search new magnetocaloric materials with large MCEs in a wide temperature range. The MCE is usually characterized in terms of the magnetic entropy change (ΔS_M) and/or adiabatic temperature change (ΔT_{ad}) in response to a magnetic field change. So far, some rare earth (*R*)–3*d* transition metal (TM) intermetallic compounds have been found to exhibit large values of ΔS_M and ΔT_{ad} around their transition temperatures because of first-order magnetic or structural phase transitions [4–7]. However, the first-order phase transition is usually accompanied with remarkable thermal and magnetic hystereses, and thus always reducing the actual efficiencies of these materials. To evaluate the refrigeration efficiency, refrigerant capacity (*RC*) has been suggested as another important criterion which depends on not only the ΔS_M value but also the width of the ΔS_M vs. *T* curve [8]. It has been pointed out that the *RC* value can be enhanced largely in some multiphase or composite materials [9–11], which would exhibit the constant MCE over a wide temperature range by adjusting the ratio of composites. On the other hand, some materials with successive magnetic transitions, such as Gd_4Co_3 [12], Ho_2In [13], *R*Ga [14,15], have been reported to present multiple ΔS_M peaks in a wide temperature region, and therefore leading to the large *RC* values. The results on these materials stimulate us to explore suitable magnetic refrigerant materials, which show multiple reversible magnetic transitions.

The magnetic properties of the intermetallic *R*NiIn compounds have been investigated extensively in the past few decades with particular interest in the field of fundamental physical properties. It is found that although these compounds form the identical crystal structure, they show different magnetic ground states and undergo complex phase transitions [16–19]. In previous studies, we have presented that *R*NiIn compounds with *R*=Gd–Er show large reversible MCEs and considerable *RC* in the temperature range of $10-100$ K [20]. Among these compounds, GdNiIn only possesses a ferromagnetic (FM) to paramagnetic (PM) transition at $T_C=98$ K. However, HoNiIn shows two successive magnetic transitions and exhibits the maximum reversible ΔS_M values of -9.5 J/kg K at $T_t=7$ K and -21.7 J/kg K at $T_C=20$ K for a magnetic field change of 5 T, respectively. These two ΔS_M peaks overlap partly, giving rise to a high value of refrigerant capacity (*RC*=341 J/kg at 5 T) over a wide temperature range. To further understand the physical properties of MCE contributed by

* Corresponding authors. Tel.: +86 10 82648085; fax: +86 10 82649485.
E-mail addresses: zhanghuxt@aphy.iphy.ac.cn (H. Zhang), shenbg@aphy.iphy.ac.cn (B.G. Shen).

0038-1098/$ - see front matter © 2012 Elsevier Ltd. All rights reserved.
http://dx.doi.org/10.1016/j.ssc.2012.06.029

different magnetic transitions and find an effective way to enhance MCE, in present work, we extend the study on the magnetic and magnetocaloric properties of $Gd_{1-x}Ho_xNiIn$ ($x=0-1$) compounds systematically.

2. Experiments

The polycrystalline $Gd_{1-x}Ho_xNiIn$ ($x=0$, 0.2, 0.4, 0.5, 0.6, 0.8, 1) samples were synthesized by arc-melting appropriate proportions of constituent components with the purity better than 99.9 wt% in a water-cooled copper hearth under purified argon atmosphere. The ingots were melted several times with the samples being turned over after each melting to ensure the homogeneity. The as-cast samples were then annealed in a high-vacuum quartz tube at 1073 K for 7–10 day. Powder X-ray diffraction (XRD) measurements were performed at room temperature by using Cu K_α radiation. The Rietveld refinement based on the XRD patterns was carried out to identify the crystal structure and the lattice parameters using the LHPM Rietica software [21]. Magnetizations and ac susceptibilities were measured by employing a commercial superconducting quantum interference device (SQUID) magnetometer, model MPMS-7 from Quantum Design Inc. The specific heat was measured by using a physical property measurement system (PPMS) from Quantum Design.

3. Results and discussion

Fig. 1 shows the observed and refined powder XRD patterns of GdNiIn compound. The XRD investigation reveals that all the $Gd_{1-x}Ho_xNiIn$ ($x=0-1$) compounds crystallize in a single phase with the ZrNiAl-type hexagonal structure (space group $P\bar{6}2m$). Moreover, it is clearly seen from the inset of Fig. 1 that the Bragg reflections shift continuously towards high angle, indicating that the lattice parameters of the compounds decrease with the increase of Ho content. The lattice parameters and densities determined from the Rietveld refinement based on the XRD patterns are listed in Table 1. It is noticed that the lattice parameters and unit cell volumes decrease while the densities of the samples increase almost linearly with increasing Ho

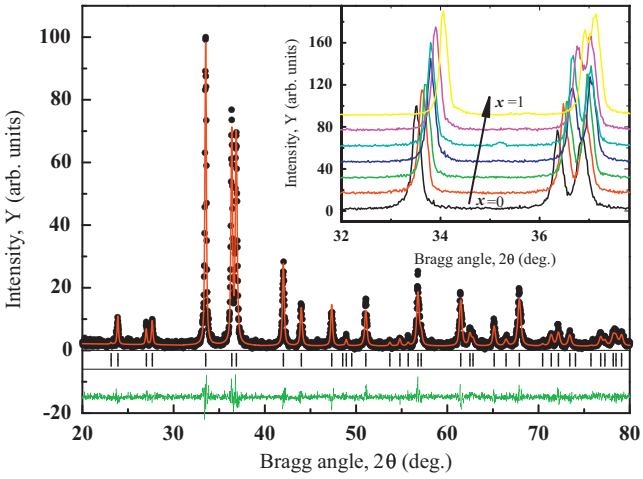

Fig. 1. The observed (dots) and calculated intensities (line drawn through the data points) of the refined powder X-ray diffraction pattern of GdNiIn compound at room temperature. The short vertical bars indicate the Bragg peak positions of ZrNiAl-type hexagonal structure. The curve at the bottom shows the difference between the observed and calculated intensities. The inset shows a close view of the XRD patterns in the angle range of 32°–38° for $Gd_{1-x}Ho_xNiIn$ ($x=0-1$, bottom-up) compounds.

Table 1
The lattice parameters, unit cell volumes and densities of $Gd_{1-x}Ho_xNiIn$ ($x=0-1$) compounds obtained from the Rietveld refinements.

x	$a=b$ (Å)	c (Å)	V (Å^3)	ρ (g/cm^3)
0	7.4386(5)	3.8372(3)	183.8(7)	8.786
0.2	7.4312(4)	3.8188(3)	182.6(3)	8.988
0.4	7.4182(4)	3.8042(3)	181.3(4)	9.168
0.5	7.4137(4)	3.7958(3)	180.6(7)	8.972
0.6	7.4119(5)	3.7869(3)	180.1(7)	9.406
0.8	7.4076(4)	3.7662(3)	178.9(7)	9.521
1	7.4007(4)	3.7498(2)	177.8(1)	9.478

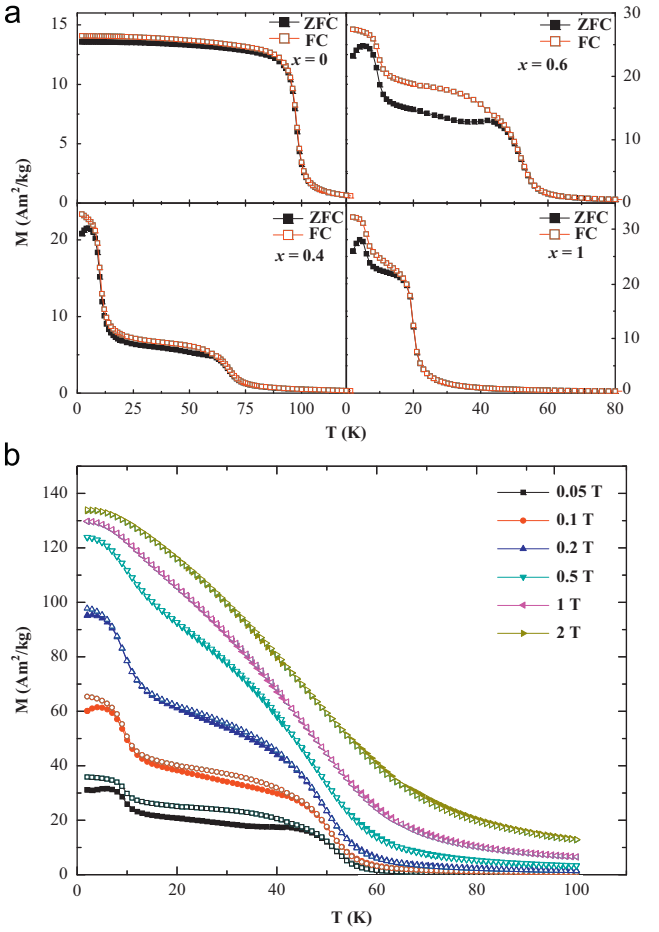

Fig. 2. (a) Temperature dependence of the magnetization of $Gd_{1-x}Ho_xNiIn$ ($x=0$, 0.4, 0.6, 1) compounds measured in a magnetic field of 0.05 T during ZFC (solid symbols) and FC (open symbols) cycles. (b) Temperature dependences of the ZFC and FC magnetizations of $Gd_{0.4}Ho_{0.6}NiIn$ in various magnetic fields.

content. This is attributed to the smaller ionic radius and larger density of Ho compared to that of Gd.

Fig. 2(a) shows the temperature (T) dependences of zero-field-cooling (ZFC) and field-cooling (FC) magnetizations (M) for $Gd_{1-x}Ho_xNiIn$ ($x=0$, 0.4, 0.6, 1) compounds in a magnetic field of 0.05 T. It is interesting to note that all the compounds, except GdNiIn, exhibit an anomaly around $T_t = 7-9$ K, which may be a spin-reorientation transition. More details about this phenomenon will be addressed later. In addition, an obvious difference between the ZFC and FC curves appears below Curie temperature (T_C) in Ho-rich compounds, which may be due to the domain wall pinning effect as usually found in materials with low ordering temperature and high anisotropy [22,23]. The introduction of Ho atoms leads to lower ordering temperature and higher anisotropy

Table 2
Magnetic transition temperatures (T_t and T_C), paramagnetic Curie temperatures (θ_P), effective magnetic moments (μ_{eff}), the maximum values of magnetic entropy change ($-\Delta S_M$) and refrigerant capacity (RC) values for a magnetic field change of 5 T in the $Gd_{1-x}Ho_xNiIn$ ($x=0-1$) system.

x	T_t (K)	T_C(K)	θ_P (K)	μ_{eff} (μ_B)		$-\Delta S_M$ (at T_t) (J/kg K)	$-\Delta S_M$ (at T_C) (J/kg K)	RC (J/kg)
				Exp	Theor			
0	–	98	101	7.96	7.94	–	7.1	326
0.2	7	81	73	8.69	8.47	2.5	7.4	322
0.4	9	67	57	9.15	9.00	3.9	7.4	232
0.5	9	59	50	9.42	9.27	5.6	7.8	254
0.6	9	52	43	9.74	9.54	6.0	10.0	443
0.8	7	34	28	10.15	10.07	7.8	13.8	432
1	7	20	18	10.61	10.60	9.5	21.7	341

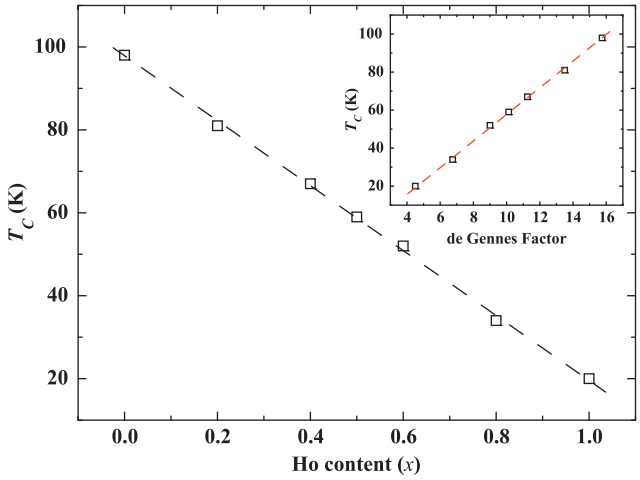

Fig. 3. The Ho content dependence of Curie temperature (T_C) in the $Gd_{1-x}Ho_xNiIn$ ($x=0-1$) compounds. The inset shows the T_C as a function of de Gennes factor.

associated with complex magnetic structure in these compounds, and thus the pinning effect becomes larger. In ZFC mode, the thermal energy at low temperature is not strong enough to overcome the energy barriers of domain walls, and this leads to the low magnetization. Fig. 2(b) shows the temperature dependences of the ZFC and FC magnetizations of $Gd_{0.4}Ho_{0.6}NiIn$ under different magnetic fields. It is seen that the magnetization between T_t and T_C remains almost constant, and two successive magnetic phase transitions can be observed clearly in low fields. With the increase of magnetic field, the magnetization below T_C enhances largely and the low-temperature transition vanishes gradually, as observed previously in HoNiIn compound [20]. In addition, it is also found that the discrepancy between ZFC and FC curves becomes smaller with increasing magnetic field. These facts indicate that the application of high magnetic field would reduce the anisotropy and depress the spin-reorientation in Ho-based compounds. The values of Curie temperature T_C, which are defined as the minimum in dM/dT vs. T curve, are summarized in Table 2. It can be seen from Fig. 3 that T_C decreases linearly from 98 K to 20 K with Ho concentration x increasing from 0 to 1. It has been reported that the magnetic ordering temperatures of RNiIn system are proportional to the de Gennes factor [24]. The de Gennes factor G for the alloy containing two lanthanide ions can be obtained as

$$G=(1-x)(g_{Gd}-1)^2J_{Gd}(J_{Gd}+1)+x(g_{Ho}-1)^2J_{Ho}(J_{Ho}+1) \quad (1)$$

where x is the concentration of Ho ions, g is the Lande splitting factor (e.g., $g_{Gd}=2$ and $g_{Ho}=1.25$), J is the total angular momentum of the corresponding magnetic ions (e.g., $J_{Gd}=3.5$ and $J_{Ho}=8$) [25]. The inset of Fig. 3 presents the T_C vs. de Gennes factor curve, and it is shown that T_C increases monotonously with respect to the de Gennes factor. This fact indicates that the decrease of T_C is due to the de Gennes factor of Ho being lower than that of Gd.

Fig. 4 shows the specific heat (C_p) curve of HoNiIn in a zero field. It also confirms that another phase transition, besides the FM-PM transition at $T_C=20$ K, is present at low temperature of 5 K. The as susceptibilities of HoNiIn measured in different frequencies are plotted in the inset of Fig. 4. It is found that the peak position of χ' does not shift to higher temperature with the variation of frequency, suggesting that the low-temperature phase transition is not related to the spin-glass or superparamagnetic systems. However, similar phenomenon has also been observed in other Ho-based intermetallic compounds [23–27]. For example, the neutron diffraction studies have shown that the magnetic structure of HoNiAl consists of both FM and AFM components. The FM components always stay along the c-axis. However, the AFM components of Ho moments are parallel to the c-axis above 5 K, and they are oriented to lie in the basal plane below 5 K [28]. Therefore, we assume that the low-temperature phase transition in the Ho-based RNiIn is also related to a spin-reorientation transition.

Above their respective Curie temperatures, the magnetic susceptibilities for all $Gd_{1-x}Ho_xNiIn$ compounds follow the Curie–Weiss law. The temperature dependences of magnetization and the inverse dc magnetic susceptibility for $Gd_{0.4}Ho_{0.6}NiIn$ compound in a magnetic filed of 1 T are plotted as an example in Fig. 5. The values of the effective magnetic moment (μ_{eff}) and paramagnetic Curie temperature (θ_P) for the $Gd_{1-x}Ho_xNiIn$ compounds, calculated from the Curie–Weiss fits of inverse magnetic susceptibility $1/\chi$ vs. T curves, are summarized in Table 2. The value of θ_P decreases from 101 K to 18 K with the increase of Ho content. In addition, the obtained μ_{eff} of each alloy is close to the theoretical value calculated by the proration of Gd^{3+} and Ho^{3+} ions, suggesting that there is nearly no interaction between Gd^{3+} and Ho^{3+} ions [29].

Magnetization isotherms of $Gd_{1-x}Ho_xNiIn$ compounds were measured in a wide temperature range under applied fields up to 5 T. Fig. 6(a) shows the magnetization isotherms of $Gd_{0.4}Ho_{0.6}$-NiIn. Around the transition temperatures, the M–H curves were measured in field increasing and decreasing modes to investigate the reversibility of the magnetic transitions. It is noted that no magnetic hysteresis is observed in each magnetization isotherm during the field increasing and decreasing cycles, revealing the perfect reversibility of the magnetic transitions. The Arrott plots

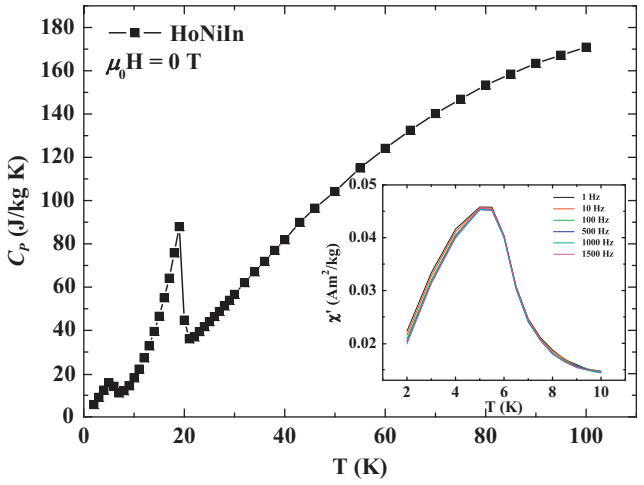

Fig. 4. Temperature dependence of the specific capacities (C_P) for HoNiIn in zero field. The inset shows the as susceptibilities of HoNiIn measured at various frequencies in a zero dc field.

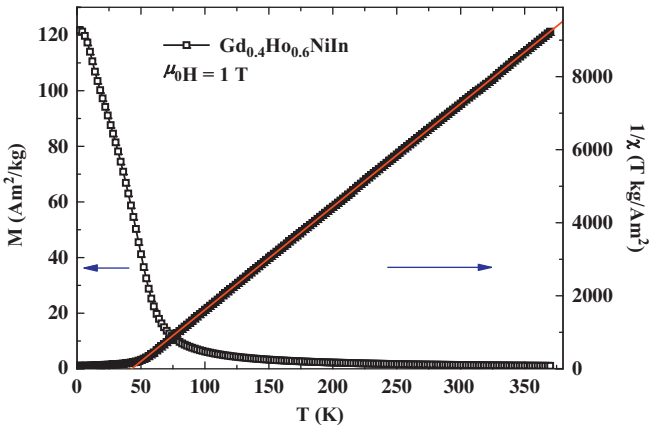

Fig. 5. The temperature dependences of magnetization and the inverse dc magnetic susceptibility for $Gd_{0.4}Ho_{0.6}NiIn$ compound under a magnetic filed of 1 T.

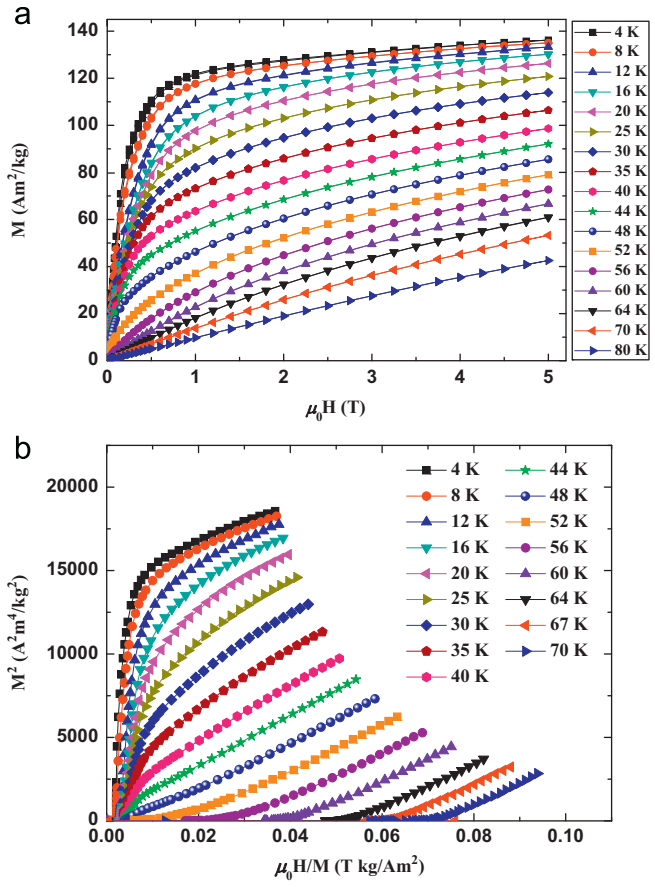

Fig. 6. (a) Magnetization isotherms of $Gd_{0.4}Ho_{0.6}NiIn$ compound in a temperature range of 4–80 K with different temperature steps. (b) Arrott plots of $Gd_{0.4}Ho_{0.6}NiIn$ in the temperature range of 4–70 K.

of $Gd_{0.4}Ho_{0.6}NiIn$ in the temperature range of 4 – 70 K are displayed in Fig. 6(b). According to Banerjee criterion [30], a magnetic transition is considered as first-order when the slope of Arrott plot is negative; whereas it is expected to be of second-order when the slope is positive. Neither inflection points nor negative slopes in the Arrott plots are observed around T_t and T_C, confirming that both successive magnetic transitions are of second-order in nature.

The magnetic entropy change ΔS_M of $Gd_{1-x}Ho_xNiIn$ compounds is calculated from the isothermal magnetization curves by using the Maxwell relation

$$\Delta S_M = \int_0^H (\partial M/\partial T)_H dH \tag{2}$$

In practice, the ΔS_M usually can be calculated using the following alternative formula

$$\Delta S_M = \sum_i \frac{M_{i+1}-M_i}{T_{i+1}-T_i}\Delta H_i \tag{3}$$

where M_i and M_{i+1} are the magnetization values at temperatures T_i and T_{i+1} in a magnetic field H_i, respectively. Fig. 7(a) shows the temperature dependence of the ΔS_M for $Gd_{1-x}Ho_xNiIn$ compounds for a magnetic field change from 0 T to 5 T. In addition to the ΔS_M peak around T_C, all the compounds with Ho atoms exhibit another ΔS_M peak centered at T_t, corresponding to the low-temperature phase transition. Table 2 lists the maximum $-\Delta S_M$ values of $Gd_{1-x}Ho_xNiIn$ compounds at respective T_t and T_C for a magnetic field change of 5 T. It is noted that the maximum value of $-\Delta S_M$ at T_C increases significantly from 7.1 J/kg K for $x=0$ to 21.7 J/kg K for $x=1$. The enhancement in $-\Delta S_M$ value is expected since free Ho^{3+} ion has higher saturation moments than that of Gd^{3+} ion. Meanwhile, the decrease in the critical temperature of Ho-rich compounds leads to the overlapping of the two ΔS_M peaks, which may also results in a larger magnetic

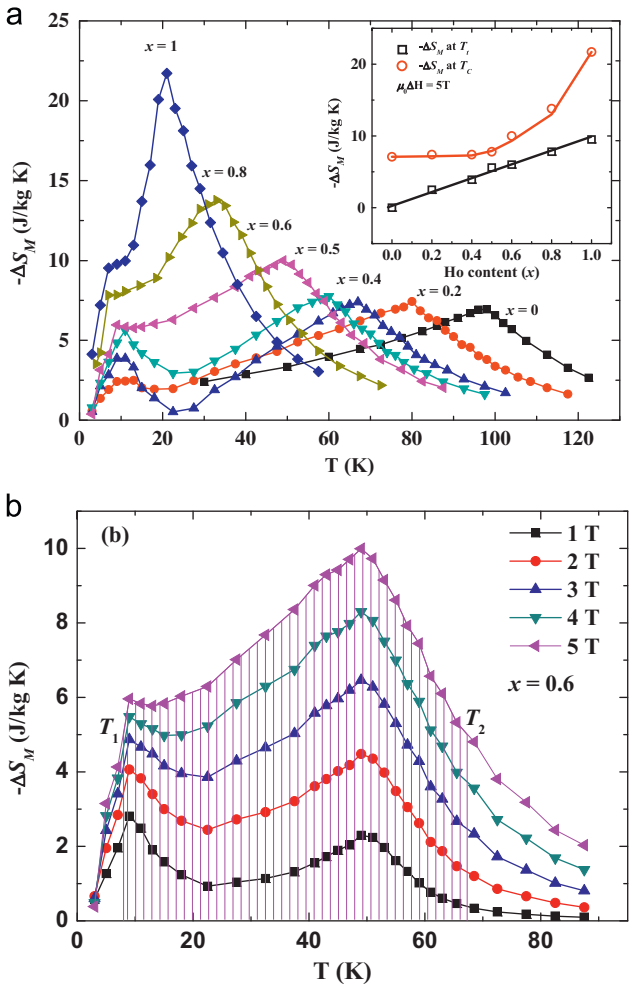

Fig. 7. (a) Temperature dependence of the isothermal magnetic entropy change ΔS_M of $Gd_{1-x}Ho_xNiIn$ ($x=0-1$) compounds for a magnetic field change from 0 T to 5 T. The inset shows the values of ΔS_M at T_t and T_C as a function of Ho content. (b) Magnetic entropy change of $Gd_{0.4}Ho_{0.6}NiIn$ as a function of temperature for different magnetic field changes. The shaded area represents the refrigerant capacity (*RC*) for a magnetic field change from 0 T to 5 T.

entropy change. In addition, it is seen from the inset of Fig. 7(a) that the maximum $-\Delta S_M$ value at T_t increases almost linearly with the increase of Ho content, which implies that the ΔS_M at low temperature is contributed mainly by the spin-reorientation transition of Ho moments. On the other hand, the ΔS_M around T_C originates from the contribution of both Gd and Ho magnetic moments, thus the Ho concentration dependence of the $-\Delta S_M$ around T_C deviates from linear relationship. In addition, it is noticed that the ΔS_M peak at T_C shifts towards lower temperature with increasing Ho content while the ΔS_M peak at T_t remains around 7 K, leading to partly overlapping of the two successive ΔS_M peaks.

It is known that the magnetic entropy change is not the only parameter to identify the potentiality of a magnetic refrigerant. The refrigerant capacity (*RC*) value is considered as another important measure of how much heat is transferred between the hot and cold ends in an ideal refrigeration cycle. From the viewpoint of practical applications, a large *RC* over a wide temperature range is favorable to an active magnetic refrigeration cycle. The *RC* values of $Gd_{1-x}Ho_xNiIn$ are estimated by using the following approach suggested by Gschneidner et al. [8]:

$$RC = \int_{T_1}^{T_2} |\Delta S_M| dT \quad (4)$$

where T_1 and T_2 are the temperatures corresponding to both sides of the half-maximum value of $-\Delta S_M$ peak, respectively. The *RC* values of $Gd_{1-x}Ho_xNiIn$ compounds thus obtained for a field change of 5 T are listed in Table 2. It is noted that the $Gd_{0.4}Ho_{0.6}$-NiIn exhibits the largest *RC* value of 443 J/kg for a field change of 5 T in this series of compounds, which is ~36% higher than that of GdNiIn (*RC*=326 J/kg). Moreover, the *RC* value increases more than one time from 82 J/kg for GdNiIn to 179 J/kg for $Gd_{0.4}Ho_{0.6}NiIn$ under a low field change of 2 T, which is advantageous to practical applications since a magnetic field of 2 T can be realized by a permanent magnet. Fig. 7(b) displays the temperature dependence of the ΔS_M of $Gd_{0.4}Ho_{0.6}NiIn$ compound for different magnetic field changes up to 5 T. It can be clearly seen that the two successive ΔS_M peaks overlap partly, expanding the working temperature range of $Gd_{0.4}Ho_{0.6}NiIn$ compound, i.e., its full width at half-maximum value of $-\Delta S_M$ peak, $\delta T_{FWHM}^S = T_2 - T_1$, is obtained to be 60 K. Therefore, the highest *RC* of $Gd_{0.4}Ho_{0.6}NiIn$ is attributed to the relatively broad distribution of large MCE, which is caused by the combined contribution of two successive magnetic transitions.

4. Conclusions

In summary, we have studied experimentally the crystal structure, magnetic and magnetocaloric properties of $Gd_{1-x}Ho_x$-NiIn compounds. The T_C decreases linearly with the increase of Ho content, which is due to the lower de Gennes factor. The temperature dependences of magnetization and heat capacity show that all the compounds, except GdNiIn, undergo a phase transition at low temperature of 7 – 9 K. This low-temperature magnetic transition is speculated to be the spin-reorientation transformation, as observed in other Ho-based intermetallic compounds. The maximum value of $-\Delta S_M$ increases largely with increasing Ho concentration. Among this series of $Gd_{1-x}Ho_xNiIn$ compounds, $Gd_{0.4}Ho_{0.6}NiIn$ exhibits a relatively large $-\Delta S_M$ of 10 J/kg K and the highest *RC* value of 443 J/kg for a magnetic field change of 5 T, which is due to the combined contribution of two successive transitions in a wide temperature range. Our results suggest that the suitable working temperature and large MCE properties can be realized by adjusting the ordering temperatures of magnetic materials with successive magnetic transitions.

Acknowledgements

This work was supported by the National Natural Science Foundation of China, the Knowledge Innovation Project of the Chinese Academy of Sciences, the Hi-Tech Research and Development program of China, and China Postdoctoral Science Foundation Funded Project.

References

[1] C.B. Zimm, A. Jastrab, A. Sternberg, V.K. Pecharsky, K.A. Gschneidner Jr., M. Osborne, I. Anderson, Adv. Cryog. Eng. 43 (1998) 1759.
[2] K.A. Gschneidner Jr., V.K. Pecharsky, A.O. Tsokol, Rep. Prog. Phys. 68 (2005) 1479.
[3] A.M. Tishin, Y.I. Spichkin, The Magnetocaloric Effect and its Applications in: J.M.D. Coey, D.R. Tilley, D.R. Vij (Eds.), Institute of Physics Publishing, Bristol, 2003.
[4] H. Wada, Y. Tanabe, M. Shiga, H. Sugawara, H. Sato, J. Alloys Compd. 316 (2001) 245.
[5] A. Giguere, M. Foldeaki, W. Schnelle, E. Gmelin, J. Phys. Condens. Matter 11 (1999) 6969.
[6] A. Fujita, S. Fujieda, K. Fukamichi, H. Mitamura, T. Goto, Phys. Rev. B 65 (2002) 014410.
[7] B.G. Shen, J.R. Sun, F.X. Hu, H.W. Zhang, Z.H. Cheng, Adv. Mater. 21 (2009) 4545.
[8] K.A. Gschneidner Jr., V.K. Pecharsky, A.O. Pecharsky, C.B. Zimm, Mater. Sci. Forum 315-317 (1999) 69.
[9] A. Chaturvedi, S. Stefanoski, M.H. Phan, G.S. Nolas, H. Srikanth, Appl. Phys. Lett. 99 (2011) 162513.
[10] R. Caballero-Flores, V. Franco, A. Conde, K.E. Knipling, M.A. Willard, Appl. Phys. Lett. 98 (2011) 102505.
[11] P. Alvarez, J.L.S. Llamazares, P. Gorria, J.A. Blanco, Appl. Phys. Lett. 99 (2011) 232501.
[12] Q. Zhang, B. Li, X.G. Zhao, Z.D. Zhang, J. Appl. Phys. 105 (2009) 053902.
[13] Q. Zhang, J.H. Cho, B. Li, W.J. Hu, Z.D. Zhang, Appl. Phys. Lett. 94 (2009) 182501.
[14] J. Chen, B.G. Shen, Q.Y. Dong, F.X. Hu, J.R. Sun, Appl. Phys. Lett. 95 (2009) 132504.
[15] J. Chen, B.G. Shen, Q.Y. Dong, J.R. Sun, Solid State Commun. 150 (2010) 157.
[16] R. Ferro, R. Marazza, G. Rambaldi, Z. Metallkd 65 (1974) 37.
[17] L. Gondek, J. Magn. Magn. Mater. 278 (2004) 392.
[18] L. Gondek, A. Szytula, B. Penc, J. Hernandez-Velasco, A. Zygmunt, J. Magn. Magn. Mater. 262 (2003) L177.
[19] F. Canepa, M. Napoletano, A. Palenzona, F. Merlo, S. Cirafici, J. Phys. D: Appl. Phys. 32 (1999) 2721.
[20] H. Zhang, Z.Y. Xu, X.Q. Zheng, J. Shen, F.X. Hu, J.R. Sun, B.G. Shen, J. Appl. Phys. 109 (2011) 123926.
[21] B.A. Hunter, Rietica, A Visual Rietveld Program, International Union of Crystallography Commission on Powder Diffraction Newsletter No. 20 (1998), www.rietica.org.
[22] R.D. dos Reis, L.M. da Silva, A.O. dos Santos, A.M.N. Medina, L.P. Cardoso, F.G. Gandra, J. Phys. Condens. Matter 22 (2010) 486002.
[23] N.K. Singh, K.G. Suresh, R. Nirmala, A.K. Nigam, S.K. Malik, J. Appl. Phys. 101 (2007) 093904.
[24] B. Yu., Ya.M. Tyvanchuk, L. Kalyczak, M. Gondek, A. Rams, Z. Szytula, Tomkowicz, J. Magn. Magn. Mater. 277 (2004) 368.
[25] Y.Y. Zhu, K. Asamoto, Y. Nishimura, T. Kouen, S. Abe, K. Matsumoto, T. Numazawa, Cryogenics 51 (2011) 494.
[26] G. Ehlers, H. Maletta, Z. Phys. B: Condens. Matter 101 (1996) 317.
[27] K. Pramod, K.G. Suresh, A.K. Nigam, O. Gutfleisch, J. Phys. D: Appl. Phys 41 (2008) 245006.
[28] P. Javorsky, P. Burlet, E. Ressouche, V. Sechovsky, G. Lapertot, J. Magn. Magn. Mater. 159 (1996) 324.
[29] B.J. Korte, V.K. Pecharsky, K.A. Gschneidner Jr., J. Appl. Phys. 84 (1998) 5677.
[30] S.K. Banerjee, Phys. Lett. 12 (1964) 16.